

Optical Bloch oscillation and Zener tunneling in an array of cylindrical waveguides. Numerical simulation.

Polishchuk I. Ya.^{1,2}, Gozman M. I.¹, Polishchuk Yu. I.²

¹ *RRC Kurchatov Institute, Kurchatov Sq., 1, 123182 Moscow, Russia*

² *Moscow Institute of Physics and Technology, 141700,
9, Institutskii per., Dolgoprudny, Moscow Region, Russia*

Abstract

We investigate optical Bloch oscillation, Zener tunneling and breathing modes in arrays of optical waveguides. We perform a new method of calculation based on the multiple scattering formalism. To demonstrate Bloch oscillation and breathing modes, we consider a planar array of parallel cylindrical waveguides with the refractive index gradually varying across the array. We demonstrate that the form of Bloch oscillation may be predicted by means of dispersion law analysis. To demonstrate Zener tunneling, we consider a planar array of cylindrical waveguides of two types situated by turn. The band structure of this array contains two bands separated by a narrow gap. If the refractive indices of waveguides gradually vary across the array, the Zener tunneling leads to the Bloch-Zener oscillation.

PACS numbers:

I. INTRODUCTION

Nowadays, much attention is devoted to arrays of evanescently coupled optical waveguides which are both of the fundamental and practical interest. These arrays are useful in integrated optical circuits and other micro- and nanooptical devices, such as optical filters and near-field microscopes.

The periodic arrays of optical waveguides represent the particular case of low-dimensional photonic crystal structures. The general feature of such systems is the existence of photonic band structure [1] that is analogous to the electron band structure in solids. Therefore some effects in optical lattices may be analogous to some phenomena in solids [2, 3]. In this work we consider optical counterparts of Bloch oscillation and Zener tunneling.

Around 1930's it was predicted that an electric field applied to a crystal should induce an oscillatory motion of the electrons, known as Bloch oscillation [4, 5]. Besides, in multiband systems electrons under an external force can spontaneously transit from one band to another. This effect is known as Zener tunneling.

Optical excitations in arrays of waveguides can perform a similar effects, as it was shown in numerous theoretical [6, 7] and experimental works. The usual pattern to demonstrate the optical Bloch oscillation and Zener tunneling is a planar array of parallel waveguides with refractive index linearly varying across the array. To produce the gradual refractive index alteration, one can use the thermo-optic [8–10] or electro-optic effects [11]. The other pattern is an array of waveguides of the same refractive indices, but of different thickness [12]. Sometimes array of identical gently curved waveguides is used [13–15].

The optical excitation coupled into such array propagates along the direction of waveguides oscillating in the transverse direction, so the propagation way of the excitation takes the sinusoidal form. This phenomena is the optical counterpart of electronic Bloch oscillation in solids. The effect of optical Bloch oscillation can be practically used in different optical devices for light steering.

The optical counterpart of Zener tunneling may take place in presence of two bands separated by a gap in the band structure of the array. The superposition of Bloch oscillation and Zener tunneling causes the splitting of an optical beam into two beams propagating along different oscillating ways. This effect is known as Bloch–Zener oscillation [7, 10, 14].

In most of works, for theoretical simulation of Bloch oscillation and Zener tunneling the following system of equations is used:

$$\left(i\frac{d}{dz} + \beta_j\right) a_j(z) + \gamma \left(a_{j-1}(z) + a_{j+1}(z)\right) = 0. \quad (1)$$

Here the waveguides are assumed to be directed along the z -axis, j is the number of a waveguide, $a_j(z)$ is the amplitude of the optical excitation at the j -th waveguide, β_j is the propagation constant of the j -th waveguide, γ is the coupling constant. This system of equations is useful for the waveguides of any form, but the parameters γ and β_j should be obtained experimentally.

In this paper we use another method of theoretical simulation based on multiple scattering formalism (MSF) [16, 17]. This method is convenient for the arrays of cylindrical waveguides. Its advantage is that the radii and refractive indices of the waveguides are the only data required for the calculation, and one has not to obtain any other parameters from an experiment. Besides, this method allows to calculate the spatial distribution of electromagnetic field around waveguides and inside of them with arbitrary accuracy, as opposed to Eq. (1), that allows only to find the intensity of optical excitation near every waveguide.

The MSF is explained in Sect. II. In Sect. III we calculate the band structure of a plane array of infinite cylindrical rods. The obtained dispersion laws are used in Sect. IV for prediction of Bloch oscillation of optical beam in an array of rods with refractive index gradually varying across the array. The prediction is confirmed by the direct numerical simulation represented in Sect. V. Besides, in Sect. V the so-called breathing mode is investigated. In Sect. VI we investigate Bloch-Zener oscillation of optical beam in a plane array of rods of two types situated by turns, with gradually varying refractive indices. Finally, in Conclusion we discuss possible practical applications of the investigated optical effects and the possibility of further development of method used in this paper.

II. MULTIPLE SCATTERING FORMALISM

We consider an array of N parallel dielectric waveguides directed along the z -axis. We assume the waveguides being infinite cylindrical rods. The array is illuminated by a monochromatic wave of frequency ω . The velocity of light in free space is supposed to be unit.

The general idea of multiple scattering formalism is that near the j -th waveguide the incident wave can be represented as a linear combination of harmonics with certain values of angular momentum m and longitudinal wave vector K :

$$\begin{aligned}
\mathbf{E}_{inc}(t, \mathbf{r}) &= e^{-i\omega t} \int dK e^{iKz} \sum_{m=-\infty}^{+\infty} e^{im\phi^{(j)}} \left(p_{jm}(K) \mathbf{M}_{\omega Km}^{(1)}(r^{(j)}) - q_{jm}(K) \mathbf{N}_{\omega Km}^{(1)}(r^{(j)}) \right), \\
\mathbf{H}_{inc}(t, \mathbf{r}) &= e^{-i\omega t} \int dK e^{iKz} \sum_{m=-\infty}^{+\infty} e^{im\phi^{(j)}} \left(p_{jm}(K) \mathbf{N}_{\omega Km}^{(1)}(r^{(j)}) + q_{jm}(K) \mathbf{M}_{\omega Km}^{(1)}(r^{(j)}) \right).
\end{aligned} \tag{2}$$

Here $r^{(j)}$ and $\phi^{(j)}$ are the polar coordinates of two-dimensional vector $\mathbf{r}^{(j)} = \{x - x_j, y - y_j\}$, and x_j, y_j are the coordinates of the axis of the j -th waveguide. Coefficients $p_{jm}(K), q_{jm}(K)$ are called the partial amplitudes of the incident wave. The expressions for functions $\mathbf{M}_{\omega Km}^{(1)}(r), \mathbf{N}_{\omega Km}^{(1)}(r)$ are given in Appendix. One can see that $\left(\mathbf{N}_{\omega Km}^{(1)}\right)_z(r) = 0$, therefore harmonics containing functions $\mathbf{M}_{\omega Km}^{(1)}(r), \mathbf{N}_{\omega Km}^{(1)}(r)$ can be named TM- and TE-harmonics correspondingly.

The wave scattered by the j -th waveguide can be represented in the similar way, but the other functions $\mathbf{M}_{\omega Km}^{(2)}(r), \mathbf{N}_{\omega Km}^{(2)}(r)$ enter into the expressions instead of the functions $\mathbf{M}_{\omega Km}^{(1)}(r), \mathbf{N}_{\omega Km}^{(1)}(r)$:

$$\begin{aligned}
\mathbf{E}_{sca}^{(j)}(t, \mathbf{r}) &= e^{-i\omega t} \int dK e^{iKz} \sum_{m=-\infty}^{+\infty} e^{im\phi^{(j)}} \left(a_{jm}(K) \mathbf{M}_{\omega Km}^{(2)}(r^{(j)}) - b_{jm}(K) \mathbf{N}_{\omega Km}^{(2)}(r^{(j)}) \right), \\
\mathbf{H}_{sca}^{(j)}(t, \mathbf{r}) &= e^{-i\omega t} \int dK e^{iKz} \sum_{m=-\infty}^{+\infty} e^{im\phi^{(j)}} \left(a_{jm}(K) \mathbf{N}_{\omega Km}^{(2)}(r^{(j)}) + b_{jm}(K) \mathbf{M}_{\omega Km}^{(2)}(r^{(j)}) \right).
\end{aligned} \tag{3}$$

The coefficients $a_{jm}(K), b_{jm}(K)$ are named the partial amplitudes of the scattered wave. The functions $\mathbf{M}_{\omega Km}^{(2)}(r), \mathbf{N}_{\omega Km}^{(2)}(r)$ are also given in Appendix.

The partial amplitudes of incident and scattered waves satisfy to the following system of equations:

$$\left(S_{jm}(\omega, K) \right)^{-1} \begin{pmatrix} a_{jm}(K) \\ b_{jm}(K) \end{pmatrix} - \sum_{\substack{l=1 \\ (l \neq j)}}^N \sum_{n=-\infty}^{\infty} e^{i(n-m)\phi_{lj}} H_{n-m}(\varkappa r_{lj}) \begin{pmatrix} a_{ln}(K) \\ b_{ln}(K) \end{pmatrix} = \begin{pmatrix} p_{jm}(K) \\ q_{jm}(K) \end{pmatrix}. \tag{4}$$

Here $\varkappa = \sqrt{\omega^2 - K^2}$, r_{lj}, ϕ_{lj} are the polar coordinates of two-dimensional vector $\mathbf{r}_{lj} = \{x_j - x_l, y_j - y_l\}$, $H_n(r)$ is the Hankel function of the first kind, and $S_{jm}(\omega, K)$ is the scattering matrix for the j -th waveguide. The scattering by a cylindrical waveguide doesn't mix harmonics with different longitudinal wave vectors K and with different angular momenta m , but harmonics of TE- and TM-types mix. The formulae to calculate the scattering matrix $S_{jm}(\omega, K)$ are cited in Appendix.

System (4) allows to find partial amplitudes of waves scattered by all the waveguides of the array. The spatial distribution of field can be calculated by formulae

$$\begin{aligned}\mathbf{E}(t, \mathbf{r}) &= \mathbf{E}_{inc}(t, \mathbf{r}) + \sum_{j=1}^N \mathbf{E}_{sca}(t, \mathbf{r}), \\ \mathbf{H}(t, \mathbf{r}) &= \mathbf{H}_{inc}(t, \mathbf{r}) + \sum_{j=1}^N \mathbf{H}_{sca}(t, \mathbf{r}).\end{aligned}\tag{5}$$

The exact system (4) consists of infinite number of equations, containing infinite number of variables. The number of equations and variables can be limited, choosing some maximal absolute value of angular momentum m_{\max} and taking into account only equations and partial amplitudes with m lying in interval $-m_{\max} \leq m \leq m_{\max}$. The spatial distribution of field can be calculated with required accuracy choosing enough great m_{\max} . It was demonstrated by the direct numerical simulation, that $m_{\max} = 2$ is enough for qualitative description of optical excitation behaviour.

III. BAND STRUCTURE CALCULATION.

Consider the infinite periodic plane array of identical cylindrical waveguides. The array is situated in xz -plane, and waveguides are directed along z -axis. The distance between two adjacent waveguides is a . Below we discuss the eigenmodes of this array and describe the method of band structure calculation.

The system of equations for eigenmodes has the left-hand side coinciding with that in system (4), and its right-hand side is zero.

$$\left(S_{jm}(\omega, K)\right)^{-1} \begin{pmatrix} a_{jm}(K) \\ b_{jm}(K) \end{pmatrix} - \sum_{\substack{l=-\infty \\ (l \neq j)}}^{+\infty} \sum_n e^{i(n-m)\phi_{lj}} H_{n-m}(\kappa r_{lj}) \begin{pmatrix} a_{ln}(K) \\ b_{ln}(K) \end{pmatrix} = 0.\tag{6}$$

Since the array is planar, $r_{lj} = a|l - j|$, $\phi_{lj} = 0$ for $j > l$ and $\phi_{lj} = \pi$ for $j < l$.

The eigenmodes of an infinite periodical array take the form of Bloch waves characterized by the transversal quasi-wave vector k ($-\pi/a < k \leq \pi/a$):

$$a_{jm}(K) = a_m(k, K) e^{ikaj}, \quad b_{jm}(K) = b_m(k, K) e^{ikaj}.\tag{7}$$

Substituting these expressions to (6), a system of equations for $a_m(k, K)$, $b_m(k, K)$ is obtained:

$$\sum_n U_{mn}(\omega, k, K) \begin{pmatrix} a_n(k, K) \\ b_n(k, K) \end{pmatrix} = 0, \quad (8)$$

where

$$U_{mn}(\omega, k, K) = \left(S_m(\omega, K) \right)^{-1} \delta_{mn} - \sum_{j=1}^{+\infty} \left(e^{-ikaj} + (-1)^{n-m} e^{ikaj} \right) H_{n-m}(\varkappa aj), \begin{pmatrix} 1 & 0 \\ 0 & 1 \end{pmatrix}. \quad (9)$$

The angular momentum takes values $-m_{\max} \leq m \leq m_{\max}$, so (8) is a homogeneous linear system of $4m_{\max} + 2$ equations with the same number of variables. If this system is represented in matrix form, its matrix $U(\omega, k, K)$ is composed of $(2m_{\max} + 1)^2$ matrices $U_{mn}(\omega, k, K)$. The system (8) possesses a nontrivial solution when the matrix $U(\omega, k, K)$ is singular: $\det U(\omega, k, K) = 0$.

Using the technic described above, we calculated the band structure for an array of cylindrical rods of unit radii ($R = 1$) made of GaAs (refractive index $n_r = 3.5$). The rods are situated next to each other, so the period of the array is $a = 2R = 2$. We calculated the dependence of longitudinal wave vector K on transverse quasi-wave vector k for a fixed frequency $\omega = 0.7\pi/a$ (below we will use the term ‘‘dispersion law’’ for the dependence $K(k)$). The approximation $m_{\max} = 2$ was used. It was shown by the direct numerical simulation, that for the chosen m_{\max} the dispersion law $K(k)$ can be found accurate within 2%. The dispersion curves $K(k)$ are presented at Fig. 1.

In Fig. 1 several dispersion curves corresponding to several different bands are illustrated. Below we consider one of the bands, that is noted by letter ‘‘A’’. This band is convenient for further investigation, since it doesn’t overlap with other bands.

Since the parameters K and k of eigenmodes are connected by the dispersion laws, one of arguments in notations $a_m(k, K)$, $b_m(k, K)$ for partial amplitudes is unnecessary, so below the partial amplitudes are denoted $a_m(K)$, $b_m(K)$.

IV. BLOCH OSCILLATION PREDICTION ON BASIS OF DISPERSION LAW.

Below we consider the Gaussian beam propagating in the array of waveguides. The partial amplitudes describing this excitation are represented by formulae

$$\begin{aligned} a_m(K) &= a_m e^{-\tau^2 (K-K_0)^2}, \\ b_m(K) &= b_m e^{-\tau^2 (K-K_0)^2}. \end{aligned} \quad (10)$$

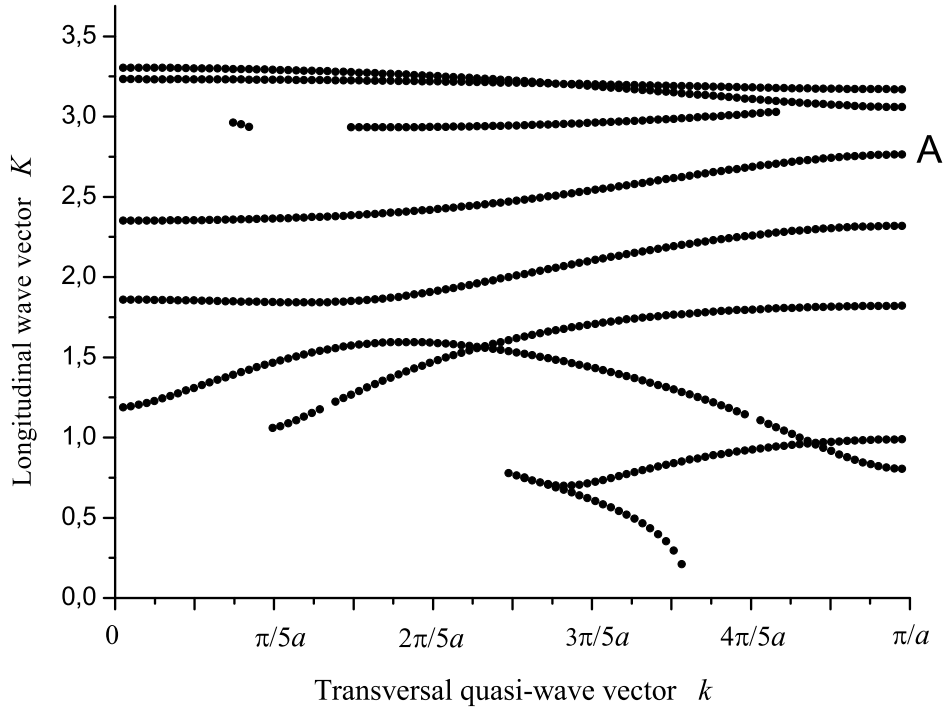


Figure 1: Dispersion curves $K(k)$.

In this case the field distribution takes the form

$$\begin{aligned}
 \mathbf{E}(t, \mathbf{r}) &= e^{-i\omega t} \mathbf{u}(\mathbf{r}) \exp \left\{ -\frac{(x/v - z)^2}{4\tau^2} + i k_0 x + i K_0 z \right\}, \\
 \mathbf{H}(t, \mathbf{r}) &= e^{-i\omega t} \mathbf{v}(\mathbf{r}) \exp \left\{ -\frac{(x/v - z)^2}{4\tau^2} + i k_0 x + i K_0 z \right\}.
 \end{aligned} \tag{11}$$

Here $\mathbf{u}(\mathbf{r})$, $\mathbf{v}(\mathbf{r})$ are the functions periodically depending on x , k_0 is connected with K_0 by the dispersion law, $K_0 = K(k_0)$, and $v = dK/dk(k_0)$. The formulae (11) are correct for enough large values of τ .

It follows from Eqs (11), that in the periodical array of identical waveguides the optical excitation propagates along the straight line $x(z) = vz$, and the direction of propagation is defined by the dispersion law $K(k)$.

But the situation changes dramatically, if the optical characteristics of waveguides (such as thickness or refractive index) gradually vary across the array.

One can mentally divide the array to sections much wider than the optical beam, but enough narrow for one could assume the waveguides into a section to be identical. One can attribute

a local dispersion law $K(k)$ to every section. Therefore, the direction of the beam propagation should be different in different sections, and the propagation way of optical excitation should be curved. A certain form of the propagation way can be predicted by calculating the dispersion law for arrays with different refractive indices of the waveguides.

For example, consider an array of $N = 100$ cylindrical rods of unite radii. The refractive index of a rod in the middle of the array ($j = 50$) is $n_r^{50} = 3.5$, and the difference between the refractive indices of two adjacent waveguides is $n_r^j - n_r^{j+1} = 0.01$, i. e.

$$n_r^j = 3.5 - 0.01(j - 50) \quad (12)$$

The section at the middle of the array is similar to the array considered in the previous section. So, we choose the parameters of optical beam according to the dispersion curve represented in Fig. 1 and marked by letter “A”. The band corresponding to that dispersion curve lies in the range $2.35 < K < 2.78$, so we choose $K_0 = 2.565$ exactly at the middle of the band. The frequency of the excitation $\omega = 0.35\pi$.

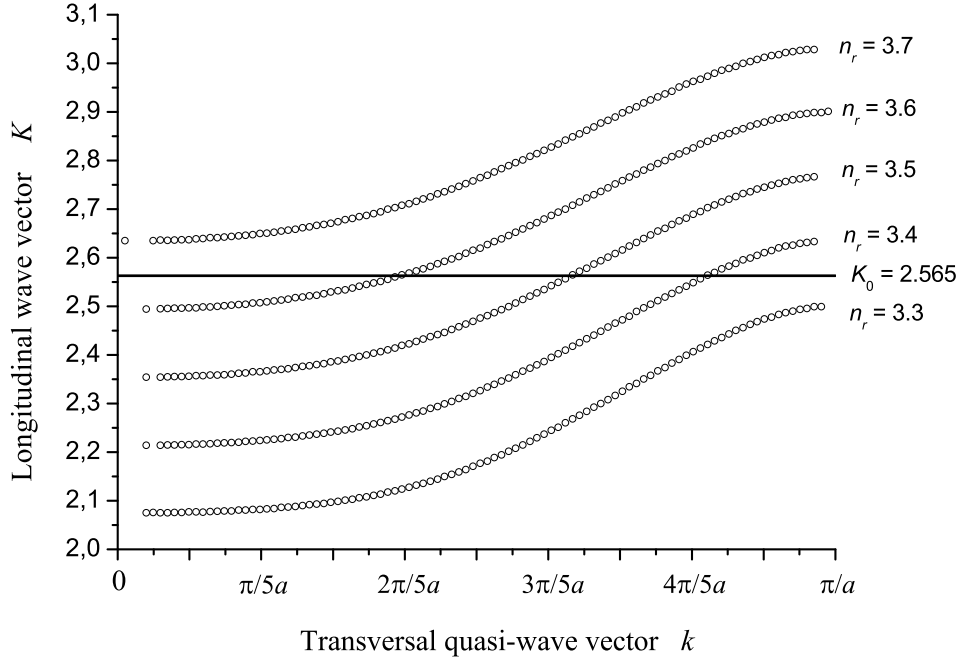


Figure 2: Dispersion laws for different refractive indices. The straight line corresponds to $K = 2.565$.

If the refractive index changes, the dispersion curve “A” shifts, as it is shown in Fig. 2. We have

found that the longitudinal wave-vector K_0 lies into the band “A” if the refractive index varies in the interval $3.35 < n_r < 3.65$. Therefore, the optical excitation can propagate in a part of the array where the refractive indices of waveguides belong to the mentioned interval, i.e. between the 35-th and 65-th waveguides.

So, we have predicted the amplitude of Bloch oscillation. But one can also predict the period of Bloch oscillation and the way of optical beam propagation. For this purpose, the value $v = dK/dk$ for K_0 for different values of refractive index n_r should be calculated. For the obtained dependence the notation $v(n_r)$ will be used. The way $x(z)$ of optical beam propagation is determined by the differential equation

$$\frac{dx}{dz} = v\left(n_r(x)\right), \quad (13)$$

where the function $n_r(x)$ is obtained by the interpolation of dependence of the waveguide refractive index n_r^j on the waveguide number j :

$$n_r(x) = 3.5 - 0.01 \left(\frac{x}{a} - 50\right). \quad (14)$$

Eq. (13) can be integrated numerically. The way of optical beam propagation, obtained from this equation, has the form of periodical oscillation, as represented in Fig. 3. The period of the obtained oscillation is $\Delta z \approx 220a = 440$ (remind that $a = 2$).

V. DIRECT CALCULATION OF BLOCH OSCILLATION AND BREATHING MODE.

In this section we represent the results of direct calculation of Gaussian beam propagation, based on numerical solution of Eq. 4. We consider the same array as in the previous section. The array is illuminated by an incident wave that is defined by partial amplitudes

$$\begin{aligned} p_{jm}(K) &= p_m e^{-\tau^2 (K-K_0)^2} \exp \left\{ -\frac{a^2 (j-j_0)^2}{4\sigma^2} + ik_0 a (j-j_0) \right\}, \\ q_{jm}(K) &= q_m e^{-\tau^2 (K-K_0)^2} \exp \left\{ -\frac{a^2 (j-j_0)^2}{4\sigma^2} + ik_0 a (j-j_0) \right\}. \end{aligned} \quad (15)$$

This incident wave illuminates the finite area of the array. The parameters σ and τ define the width of the illuminated area along x -axis and z -axis correspondingly. We take $j_0 = 50$, i. e. the incident wave illuminates the middle of the array. The parameters K_0 and k_0 are connected by the dispersion law marked by letter “A” in Fig. 1. We take $K_0 = 2.565$, exactly at the middle of

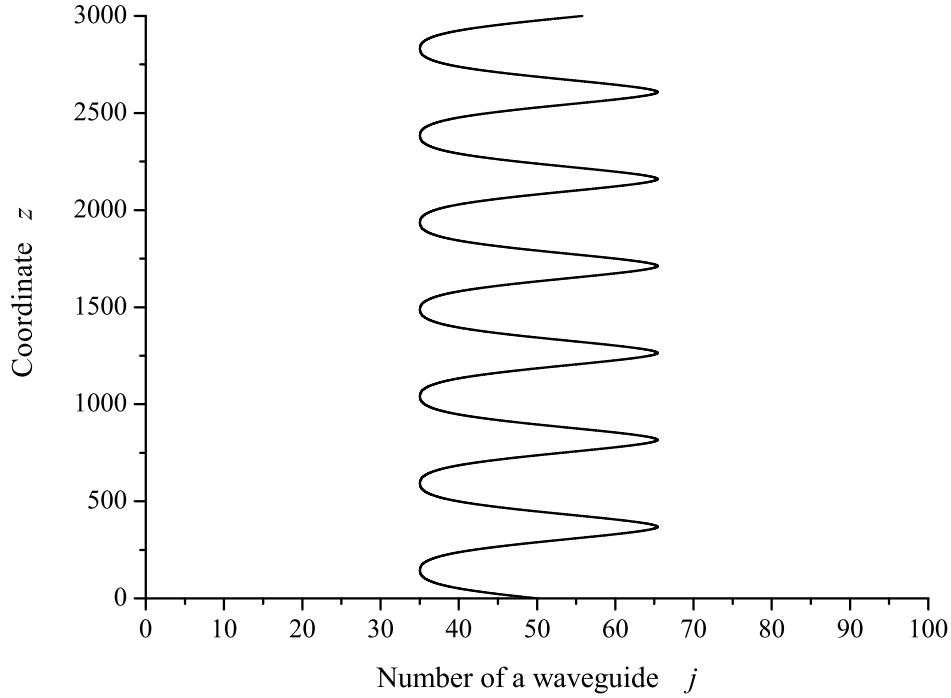


Figure 3: Optical excitation propagation way obtained by the analysis of dispersion law.

the band “A” ($2.35 < K < 2.78$), and the corresponding $k_0 = 0.989$. The parameter τ is chosen so that the peak of the function $e^{-\tau^2(K-K_0)^2}$ fits into the band “A”: $\tau = 6/\Delta K \approx 14$, where ΔK is the width of the band “A”. The parameter $\sigma = v(k_0)\tau$, where $v(k_0)$ is defined by the dispersion law: $v(k_0) = dK/dk(k_0)$. Here $v(k_0) \approx 0.5$, so $\sigma = 7$.

The parameters p_m, q_m are chosen so that the incident wave excites the eigenmodes of the array effectively. For our calculation we chose $q_0 = 1$ and all the other p_m, q_m are zeros. The computation is performed for the approximation $m_{\max} = 2$.

The result of the computation is presented in Fig. 4. As expected, the obtained way of optical beam propagation has a periodical form. It oscillates between the 35-th and 65-th waveguides, and the period of oscillation is $\Delta z = 440$. It is remarkable that the form of oscillation obtained by the numerical solution of Eq. (4) coincides exactly with that obtained by the dispersion law analysis.

Besides the Bloch oscillation, we consider the so-called breathing mode [6, 12, 14]. Such kind of optical excitation arises when only one waveguide of the array is illuminated by the incident wave.

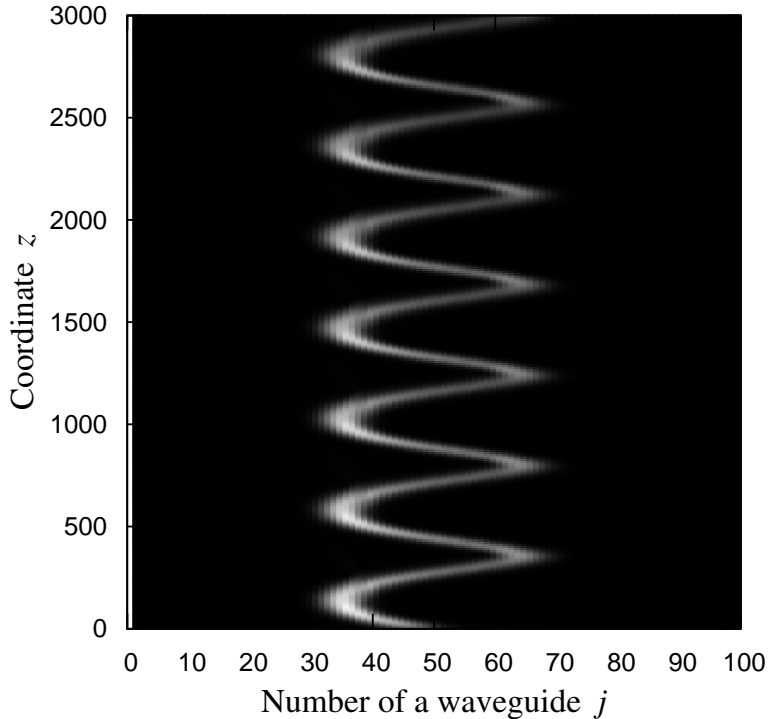


Figure 4: Optical excitation propagation.

The characteristic feature of breathing mode is the periodical spreading and focusing behaviour.

We assume that the incident wave illuminates a short section around $z = 0$ of the 50-th waveguide situated at the middle of the array. To simulate this situation, we take the partial amplitudes of the incident wave as follows: $p_{jm}(K) = 0$, $q_{jm}(K) = 0$, $q_{j0}(K) = 1$. The result of direct numerical calculation is represented in Fig. 5.

VI. BLOCH-ZENER OSCILLATION.

The optical Bloch-Zener oscillation in an array of optical waveguides can take place if the band structure consists of several bands separated by gaps. If the refractive index of waveguides gradually varies across the array, the band structures of two different sections of the array are shifted relative to each other. Therefore, the lower band of one section can overlap the upper band of another section. So, the optical beam can partially tunnel from one section to another. This

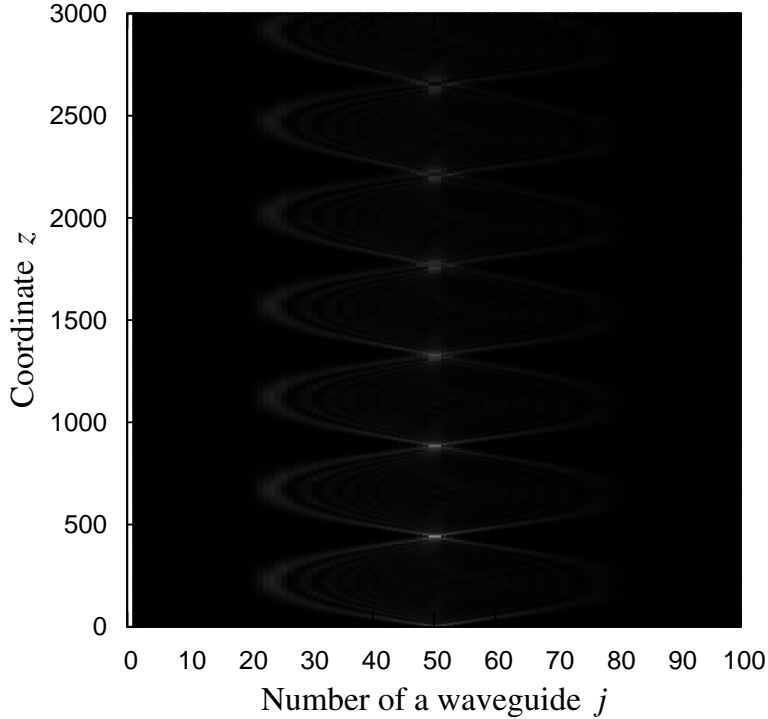


Figure 5: Breathing mode.

leads to that the optical beam divides into two beams propagating along two different oscillating ways.

To demonstrate this effect, it is convenient to consider an array with the band structure containing two bands separated with a narrow gap. We take the array of waveguides of two types situated by turns. The refraction indices of waveguides of the first and the second type are $n_{r1} = 3.5$ and $n_{r2} = 3.55$ respectively. The band structure of this array contains two bands $2.38 < K < 2.48$ and $2.54 < K < 2.8$ (we suppose the frequency $\omega = 0.35\pi$, as in previous sections).

We introduce a small variation of refraction indices of waveguides:

$$\begin{aligned} n_r^j &= 3.5 - 0.005(j - 50) \quad \text{for odd } j, \\ n_r^j &= 3.55 - 0.005(j - 50) \quad \text{for even } j. \end{aligned} \tag{16}$$

The array is illuminated by the incident wave defined by the partial amplitudes $p_{jm}(K)$, $q_{jm}(K)$,

that are given by formulae (15). The parameters K_0 , k_0 , τ , σ entering to these formulae are chosen according to the principle similar to that described in the previous section. The parameter $K_0 = 2.67$ is taken exactly at the middle of the band $2.54 < K < 2.8$, the parameter $k_0 = 0.44$ is connected to K_0 by the dispersion law $K(k)$, the value of $\tau = 23$ is taken so that the peak of the function $e^{-\tau^2(K-K_0)^2}$ entirely fits into the band $2.54 < K < 2.8$, and $\sigma = dK/dk(k_0) \tau = 10$.

The result of the calculation is represented on Fig. 6.

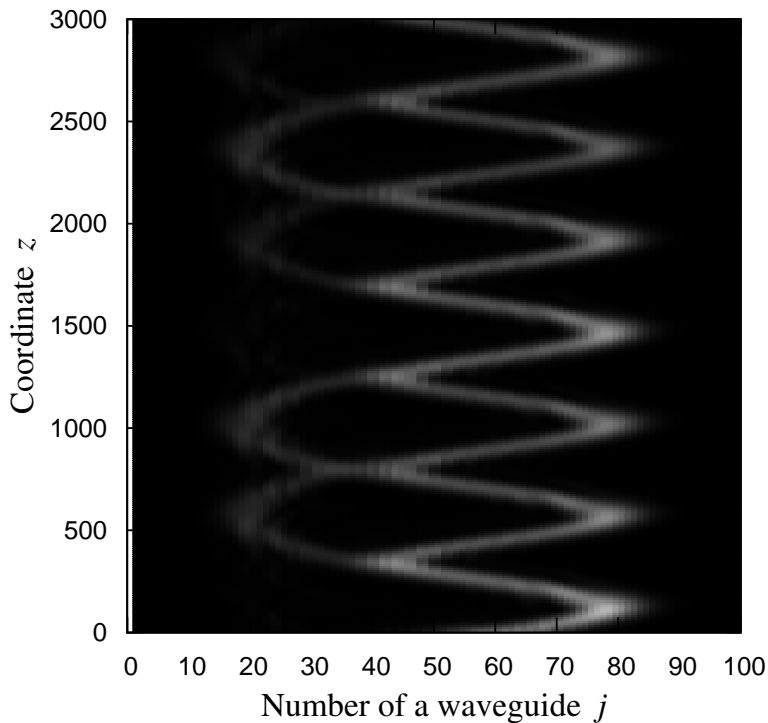


Figure 6: Bloch-Zener oscillation.

VII. CONCLUSION.

In this paper three phenomena are considered — Bloch oscillation, Bloch-Zener oscillation and breathing modes in planar arrays of optical waveguides with gradually varying refractive index. We suggest a new method to investigate this subject, based on the multiple scattering formalism. This method has several advantages over the traditional method based on Eq. (1). The MSF

allows to find the spatial distribution of field with any required accuracy, while the traditional method gives only the intensity of optical excitation. Besides, the input data for MSF are the geometrical properties of the array and refractive indices of waveguides, while the traditional method requires some data that should be obtained experimentally, such as the longitudinal wave vectors of eigenmodes of waveguides and coupling constants.

The MSF represented in this paper is convenient only for the waveguides of cylindrical form, because in this case the scattering matrix can be calculated easily. However, this method can be applied for the waveguides of another shape, but in this case it would be more difficult to calculate the scattering matrix. Besides, the scattering by noncylindrical waveguides would mix the harmonics with different angular momenta. So, if the shape of the waveguides is enough complicated, one should take into account the harmonics with enough high angular momenta, and the calculation would be difficult. At the same time, for the cylindrical waveguides it is enough to take into account the harmonics with $|m| \leq 2$, as it is shown in this work.

The considered phenomena may be useful for different optical applications, such as steering, splitting, focusing and defocusing of light. The method represented in this work allows to produce the numerical simulation without need of experimental investigation of components of optical devices.

-
- [1] J. Joannopoulos, P. R. Villeneuve, S. Fan. *Nature* **386**, 143 (1997).
 - [2] F. Lederer, G. I. Stegeman, D. N. Christodoulides, G. Assanto, M. Segev, Y. Silberberg. *Phys. Rep.* **463**, 1 (2008).
 - [3] S. Longhi. *Laser & Photon. Rev.* **3**, 243 (2009).
 - [4] F. Bloch. *Z. Phys.* **52**, 555 (1928).
 - [5] C. Zener. *Proc. R. Soc. Lond. A* **145**, 523 (1934).
 - [6] Ming Jie Zheng, Gang Wang, Kin Wah Yu. *Opt. Lett.* **35**, 3865 (2010).
 - [7] Gang Wang, Ji Ping Huang, Kin Wah Yu. *Opt. Lett.* **35**, 1908 (2010).
 - [8] T. Pertsch, P. Dannberg, W. Elflein, A. Bräuer, F. Lederer. *Phys. Rev. Lett.* **83**, 4752 (1999).
 - [9] T. Pertsch, T. Zentgraf, U. Peschel, A. Bräuer, F. Lederer. *Appl. Phys. Lett.* **80**, 3247 (2002).
 - [10] H. Trompeter, T. Pertsch, F. Lederer, D. Michaelis, U. Streppel, A. Bräuer, U. Peschel. *Phys. Rev. Lett.* **96**, 023901 (2006).

- [11] U. Peschel, T. Pertsch, F. Lederer. Opt. Lett. **23**, 1701 (1998).
- [12] R. Morandotti, U. Peschel, J. S. Aitchison, H. S. Eisenberg, Y. Silberberg. Phys. Rev. Lett. **83**, 4756 (1999).
- [13] N. Chiodo, G. Della Valle, R. Osellame, S. Longhi, G. Cerullo, R. Ramponi, P. Laporta, U. Morgner. Opt. Lett. **31**, 1651 (2006).
- [14] F. Dreisow, A. Szameit, M. Heinrich, T. Pertsch, S. Nolte, A. Tünnermann, S. Longhi. Phys. Rev. Lett. **102**, 076802 (2009).
- [15] F. Dreisow, Gang Wang, M. Heinrich, R. Keil, A. Tünnermann, S. Nolte, A. Szameit. Opt. Lett. **36**, 3963 (2011).
- [16] E. Centeno, D. Felbacq. J. Opt. Soc. Am. A **17**, 320 (2000).
- [17] K. Vynck, D. Felbacq, E. Centeno, A. I. Căbuz, D. Cassagne, B. Guizal. Phys. Rev. Lett. **102**, 133901 (2009).

APPENDIX.

1. Formulae for functions $\mathbf{M}_{\omega Km}^{(1)}(r)$ and $\mathbf{N}_{\omega Km}^{(1)}(r)$:

$$\begin{aligned} \mathbf{M}_{\omega Km}^{(1)}(r) &= \mathbf{e}_r \frac{iK}{2\kappa} \left(J_{m-1}(\kappa r) - J_{m+1}(\kappa r) \right) + \\ &+ \mathbf{e}_\phi \frac{-K}{2\kappa} \left(J_{m-1}(\kappa r) + J_{m+1}(\kappa r) \right) + \mathbf{e}_z i J_m(\kappa r), \end{aligned} \quad (17)$$

$$\begin{aligned} \mathbf{N}_{\omega Km}^{(1)}(r) &= \mathbf{e}_r \frac{\omega}{2\kappa} \left(J_{m-1}(\kappa r) + J_{m+1}(\kappa r) \right) + \\ &+ \mathbf{e}_\phi \frac{i\omega}{2\kappa} \left(J_{m-1}(\kappa r) - J_{m+1}(\kappa r) \right). \end{aligned} \quad (18)$$

Here $\kappa = \sqrt{\omega^2 - K^2}$, $J_m(x)$ is Bessel function.

2. Formulae for functions $\mathbf{M}_{\omega Km}^{(2)}(r)$ and $\mathbf{N}_{\omega Km}^{(2)}(r)$:

$$\begin{aligned} \mathbf{M}_{\omega Km}^{(2)}(r) &= \mathbf{e}_r \frac{iK}{2\kappa} \left(H_{m-1}(\kappa r) - H_{m+1}(\kappa r) \right) + \\ &+ \mathbf{e}_\phi \frac{-K}{2\kappa} \left(H_{m-1}(\kappa r) + H_{m+1}(\kappa r) \right) + \mathbf{e}_z i H_m(\kappa r), \end{aligned} \quad (19)$$

$$\begin{aligned} \mathbf{N}_{\omega K m}^{(2)}(r) = & \mathbf{e}_r \frac{\omega}{2\kappa} \left(H_{m-1}(\kappa r) + H_{m+1}(\kappa r) \right) + \\ & + \mathbf{e}_\phi \frac{i\omega}{2\kappa} \left(H_{m-1}(\kappa r) - H_{m+1}(\kappa r) \right). \end{aligned} \quad (20)$$

Here $H_m(x)$ is Hankel function of the first kind.

3. Formulae for scattering matrix:

Consider an infinite dielectric rod situated along the z -axis. The radius of the rod is R , and its refractive index n_r . It is illuminated by a monochromatic wave of frequency ω with certain longitudinal wave vector K and angular momentum m . This wave is defined by two partial amplitudes $p_m(K)$, $q_m(K)$. The scattered wave possesses the same frequency ω , longitudinal wave vector K and angular momentum m . It is defined by partial amplitudes $a_m(K)$, $b_m(K)$.

Partial amplitudes of incident and scattered waves are connected by the scattering matrix $S_m(\omega, K)$:

$$\begin{pmatrix} a_m(K) \\ b_m(K) \end{pmatrix} = S_m(\omega, K) \begin{pmatrix} p_m(K) \\ q_m(K) \end{pmatrix}. \quad (21)$$

To formulate the expression for matrix $S_m(\omega, K)$, we introduced some notations:

$$\begin{aligned} \kappa &= \sqrt{\omega^2 - K^2}, & \xi &= \kappa R, & \alpha &= K/2\kappa, & \beta &= \omega/2\kappa, \\ \kappa_i &= \sqrt{n_r^2 \omega^2 - K^2}, & \xi_i &= \kappa_i R, & \alpha_i &= K/2\kappa_i, & \beta_i &= n_r \omega/2\kappa_i, \end{aligned} \quad (22)$$

$$\begin{aligned} w_- &= J_{m-1}(\xi) - J_{m+1}(\xi), & w_0 &= J_m(\xi), & w_+ &= J_{m-1}(\xi) + J_{m+1}(\xi), \\ u_- &= H_{m-1}(\xi) - H_{m+1}(\xi), & u_0 &= H_m(\xi), & u_+ &= H_{m-1}(\xi) + H_{m+1}(\xi), \\ v_- &= J_{m-1}(\xi_i) - J_{m+1}(\xi_i), & v_0 &= J_m(\xi_i), & v_+ &= J_{m-1}(\xi_i) + J_{m+1}(\xi_i). \end{aligned} \quad (23)$$

$$\begin{aligned} M_{11} &= \begin{pmatrix} -i\alpha u_- & \beta u_+ \\ \alpha u_+ & i\beta u_- \end{pmatrix}, & M_{21} &= \begin{pmatrix} -u_0 & 0 \\ 0 & -u_0 \end{pmatrix}, \\ M_{12} &= \begin{pmatrix} in_r^2 \alpha_i v_- & -n_r^2 \beta_i v_+ \\ -\alpha_i v_+ & -i\beta_i v_- \end{pmatrix}, & M_{22} &= \begin{pmatrix} v_0 & 0 \\ 0 & n_r v_0 \end{pmatrix}, \\ N_1 &= \begin{pmatrix} i\alpha w_- & -\beta w_+ \\ -\alpha w_+ & -i\beta w_- \end{pmatrix}, & N_2 &= \begin{pmatrix} w_0 & 0 \\ 0 & w_0 \end{pmatrix}. \end{aligned} \quad (24)$$

Using the introduced notations, we write down the expression for matrix $S_m(\omega, K)$:

$$S_m(\omega, K) = \left(M_{12}^{-1} M_{11} - M_{22}^{-1} M_{21} \right)^{-1} \left(M_{12}^{-1} N_1 - M_{22}^{-1} N_2 \right). \quad (25)$$